A Cambrian island arc in the Silvretta nappe: constraints from geochemistry and geochronology

by U. Schaltegger[1], Th.F. Nägler[2], F. Corfu[3], M. Maggetti[4], G. Galetti[4] and H.G. Stosch[5]

Abstract

Mafic, intermediate and felsic polymetamorphic gneisses in the Austroalpine Silvretta nappe are traditionally called "Older Orthogneisses"; investigation of their geochemical and Nd isotopic characteristics as well as age determinations by the U–Pb zircon method revealed that this unit is heterogeneous in terms of origin, geodynamic setting and age. A dioritic protolith was emplaced in an arc-type setting 609 ± 3 Ma ago. A flasergabbro, a metagabbro with preserved magmatic textures and a metatonalite yielded U–Pb ages of 523 ± 3, 522 ± 6 and 524 ± 5 Ma, respectively. They intruded into a basement consisting of metasediments typical for active continental margin deposits and interlayered with intrusive/extrusive metabasites from a T- to P-type MORB source, but, on the other hand, occur together with coeval ophiolitic rocks. Metagabbros and metatonalites are proposed to have been formed in an island arc, either in the vicinity of an active continental margin or in a back-arc setting. The heterogeneous rock suite was subsequently involved in orogenic processes during Ordovician times and again intruded by gabbroic melts 475 Ma ago.

The studied rocks reveal the existence of an oceanic domain between Gondwana and Laurasia continental blocks prevailing over a period of more than 150 myr in the Late Proterozoic, Cambrian and Ordovician.

Keywords: geochemistry, U–Pb zircon ages, Nd characteristics, island arc, basement evolution, Silvretta nappe, Austroalpine.

1. Introduction

The Austroalpine Silvretta nappe consists of a large variety of polymetamorphic gneisses of both sedimentary and igneous origin. A series of granitic, dioritic, tonalitic, gabbroic and ultramafic gneisses has been termed Older Orthogneisses (OOG) by GRAUERT (1969). Investigation of this unit is clearly hampered by the fact that it is scattered over the whole southern part of the Silvretta nappe as isolated inliers within younger units. Previous geochemical studies revealed that the OOG unit is heterogeneous in terms of the geodynamic setting of the different members: A variety of granitic, tonalitic, dioritic and gabbroic gneiss types were shown to have no common magma source, but are compatible with a formation in an island arc setting (MAGGETTI et al., 1990; POLLER, 1994 a, b; POLLER et al., 1997). A mid-ocean ridge setting has been proposed for metaaplites interbedded in amphibolites (BERLEPSCH, 1992, 1996) and garnet-hornblende-plagioclase gneisses, whose geochemical compositions resemble those of oceanic plagiogranites derived by fractional crystallization from basic liquids (MÜLLER et al., 1996). Rocks of crustal origin comprise probably anorogenic alkali granites (MÜLLER et al., 1995) and peraluminous S-type granites and anatexites (Mönchalp augengneisses; POLLER, 1994 a, b).

The age information available so far for rocks of *intermediate and mafic* compositions is highly conflicting: Rb–Sr whole-rock data for gabbros and tonalites straddle a best-fit line with an age of

[1] Departement Erdwissenschaften, Institut für Isotopengeologie und Mineralische Rohstoffe, ETH-Zentrum, CH-8092 Zürich, Switzerland. E-mail: schaltegger@erdw. ethz.ch.

[2] Mineralogisch-Petrographisches Institut, Abt. für Isotopengeologie, Universität Bern, Erlachstrasse 9a, CH-3012 Bern, Switzerland.

[3] Royal Ontario Museum, Earth Science Department, 100 Queen's Park, Toronto, Ontario M5S 2C6, Canada.

[4] Institut de Minéralogie et Pétrographie, Université de Fribourg, Pérolles, CH-1700 Fribourg, Switzerland.

[5] Institut für Petrographie und Geochemie, Universität Karlsruhe (TH), D-76128 Karlsruhe, Germany.
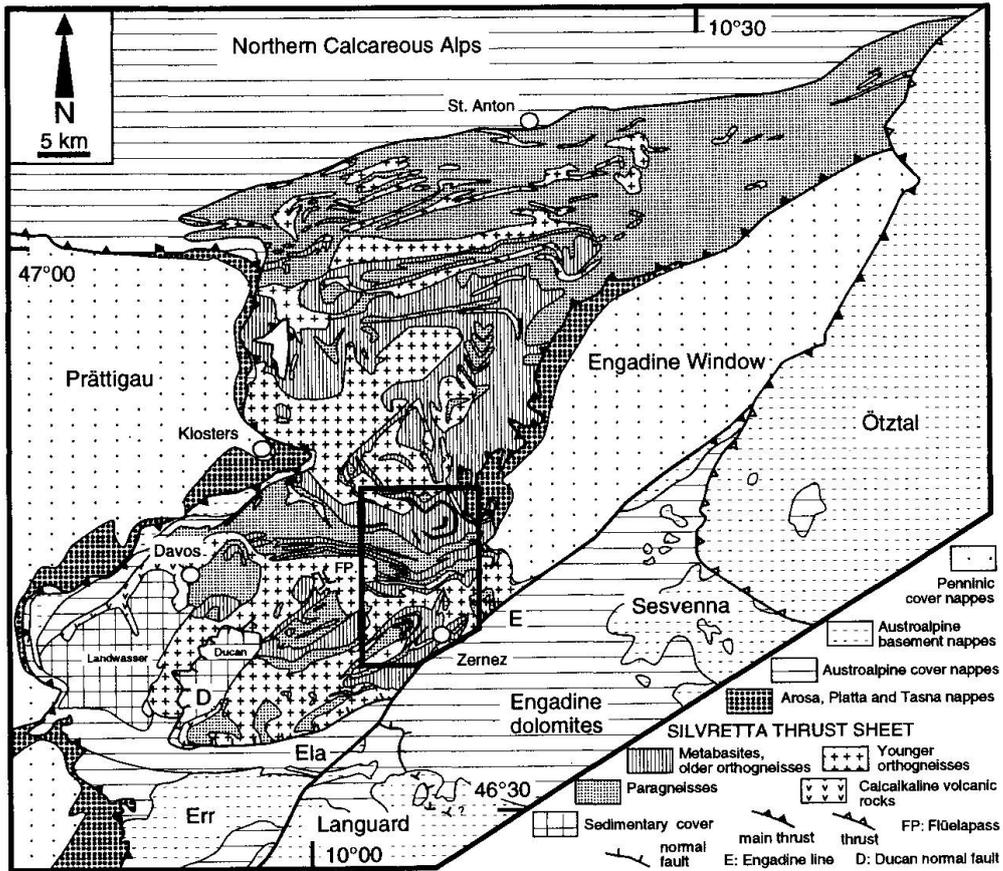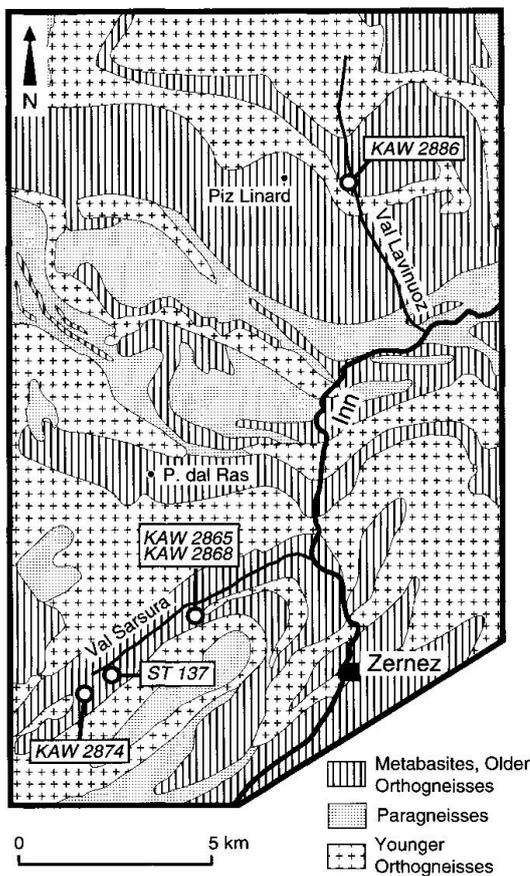
Fig. 1a

Fig. 1b

Fig. 1   (a) Geological sketch map of the Silvretta nappe (PROSPERT, 1996); enlarged area (b) shows sampling sites of dated Older Orthogneiss samples in Val Sarsura and Val Lavinuoz near Zernez.

895 Ma (MAGGETTI and FLISCH, 1993), whereas U–Pb and Pb–Pb evaporation ages (MÜLLER et al., 1995) for two calc-alkaline gneisses (biotite-hornblende gneiss, biotite-plagioclase gneiss) and an alkaline granite gneiss ranged between 519 and 533 Ma. U–Pb zircon dating of garnet-hornblende-plagioclase gneisses yielded an imprecise discordia upper intercept age of 532 ± 30 Ma, interpreted as the primary crystallization age of the igneous protoliths (MÜLLER et al., 1996). The *granitic* Mönchalp augengneisses yielded Cambrian zircon U–Pb ages at around 530 Ma (POLLER, 1994a; POLLER et al., 1997) interpreted as emplacement age. The granitic to granodioritic melts intruded a metamorphic continental basement featuring sedimentary rocks interlayered with mafic intrusives. The basement contribution is reflected by a considerable amount of xenoliths and by high Nd T_{DM} model ages of 1.7 Ga of the granitoid members (POLLER, 1994b; POLLER et al., 1997).

The aim of this work is to constrain the intrusion ages of the OOG protoliths more precisely and to propose a coherent geodynamic interpretation on the basis of geochemical and geochronological results.

2. Investigated samples

Detailed petrographic descriptions for the intermediate and basic members of the Older Orthogneisses were presented by SPAENHAUER (1932) and THIERRIN (1982, 1983) and have been summarized by MAGGETTI et al. (1990). A recent study of the gabbro-metagabbro transition was presented by BENCIOLINI (1994). MÜLLER et al. (1996) gave additional geochemical data for the gabbroic complex of the Val Sarsura. The ultramafic, gabbroic and granitic types locally preserve magmatic structures, in contrast to the strongly foliated intermediate dioritic hornblende-gneisses and tonalitic biotite-gneisses, which could possibly have formed as volcanic rocks. A plutonic origin has, however, traditionnally been assumed (MAGGETTI and FLISCH, 1993) and we therefore use the plutonic nomenclature.

Five samples covering the whole lithological range of the OOG were analyzed for whole-rock Sm and Nd, and for zircon U and Pb isotopic compositions. The samples (Fig. 1) were originally collected for the Rb–Sr whole-rock work published in MAGGETTI and FLISCH (1993) and consisted of 15 to 30 kg of fresh rock, except for ST 137, which is a handspecimen collected by THIERRIN (1983) and was used for U–Pb zircon dating only. Gabbroic and tonalitic samples originate from two

outcrops in the Val Sarsura west of Zernez with clearly visible field relationships, which would enable a coherent interpretation of the age results. A strongly retrograded eclogite, now a symplectitic garnet-amphibolite, from the same area was analyzed for Sm–Nd for the purpose of comparison with the gabbro.

KAW 2865 (Flasergabbro), Ova Sparsa, Val Sarsura, Coord. 799 675/176 200 of the Swiss topographic grid: Deformed gabbro-norite with a well developed schistosity. All transitions from the undeformed, primary isotropic magmatic texture (like in sample KAW 2868) to the flasergabbro texture can be seen in outcrop. Typical non-equilibrium assemblages are: a) tremolitic amphibole and chlorite replacing older magmatic or eclogitic phases, b) plagioclase totally replaced by "saussuritic" breakdown products, c) garnet coronas relictic from the HP-metamorphism. Flasergabbros are interpreted as products of high-pressure shearing in gabbros under eclogite-facies conditions. Deformation remained active until they reached greenschist facies.

KAW 2868 (Coarse-grained metagabbro), Ova Sparsa, Val Sarsura, Coord. 799 675/176 200: Gabbro-norite with magmatic texture and well preserved magmatic minerals such as euhedral hypersthene (up to 5 mm long), partially replaced by secondary "saussurite", diopside, strongly sericitized plagioclase, ilmenite and apatite. Quartz, biotite and minor white mica occur in interstices.

ST 137 (Gabbro pegmatite), Val Sarsura, Coord. 798 200/175 950: Leucocratic gabbronorite made up of large euhedral hypersthene crystals (up to 5 cm long), partially saussuritized plagioclase, quartz, ilmenite, apatite and pyrrhotite. They are strongly deformed in most cases, except when intruding into amphibolites.

KAW 2874 (Metatonalite), Val Sarsura, Coord. 797 540/175 200: Strongly foliated rock, consisting of partially sericitized and saussuritized plagioclase, quartz, partially chloritized biotite, amphibole and sphene.

KAW 2879 (Eclogite), Val Punt'ota, Coord. 796 500/170 625: Medium- to coarse-grained eclogite, garnet and omphacite (partially replaced by a symplectitic intergrowth of plagioclase and amphibole) in approximately equal amounts (type 2 eclogite according to MAGGETTI et al., 1987), little zoisite, amphibole and rutile.

KAW 2886 (Metadiorite), Val Lavinuoz, Coord. 802 375/186 680: Strongly foliated hornblende-plagioclase gneiss with amphibole and partially saussuritized resp. sericitized plagioclase in equal amounts, little quartz, biotite with secondary chlorite and prehnite, and secondary sphene. Contains xenoliths of amphibolite and

Tab. 1 Major and trace element concentrations of investigated rocks.

Sample	SiO$_2$	TiO$_2$	Al$_2$O$_3$	Fe$_2$O$_3$	FeO	MnO	MgO	CaO	Na$_2$O	K$_2$O	P$_2$O$_5$	L.O.I.	Sum
KAW 2865 (Flasergabbro)	52.4	2.02	18.00	1.81	6.35	0.15	5.35	8.48	3.29	0.64	0.15	1.53	100.16
KAW 2868 (Coarse-grained metagabbro)	51.9	1.93	16.97	1.51	7.30	0.16	6.45	8.49	3.01	0.66	0.17	1.29	99.85
KAW 2874 (Metatonalite)	69.8	0.29	16.34	0.70	1.50	0.05	1.24	3.89	4.54	0.88	0.08	1.12	100.46
KAW 2879 (Eclogite)	50.4	1.88	13.91	3.00	10.28	0.25	6.22	10.83	2.39	0.13	0.18	0.10	99.57
KAW 2886 (Metadiorite)	48.1	1.05	18.83	3.57	5.55	0.16	7.06	9.91	2.38	0.59	0.12	2.18	99.53

Sample	Nb	Zr	Y	Sr	Rb	Th	Ga	Zn	Cu	Ni	Cr	V	Ba
KAW 2865 (Flasergabbro)	2	73	16	354	12	n.d.	19	80	11	33	157	250	302
KAW 2868 (Coarse-grained metagabbro)	≤1	79	18	343	6	n.d.	19	83	6	37	173	266	269
KAW 2874 (Metatonalite)	≤1	123	5	300	24	n.d.	14	35	6	10	18	35	597
KAW 2879 (Eclogite)	4	92	43	122	≤1	≤1	32	122	62	55	145	425	35
KAW 2886 (Metadiorite)	≤1	35	18	399	7	n.d.	20	81	51	99	69	318	231

Analyzed by x-ray fluorescence, except for FeO (wet chemical methods); major elements in wt%, trace elements in ppm.

paragneiss; there are no indications whether it is an extrusive or intrusive rock.

3. Analytical techniques

Geochemical analyses: Bulk chemical X-ray fluorescence (XRF) analyses for major and trace elements were obtained by an automated Philips model PW 1400 sequential spectrometer; abundances of REE, Hf, Ta and Th were measured by instrumental neutron activation analysis (INAA); for analytical details see MAGGETTI et al. (1987).

U–Pb age determinations: Zircon was separated from a fraction smaller than 300 µm using standard methods. The non-magnetic zircon sub-fraction was examined under a binocular microscope and suitable grains of high purity (without cracks, turbid zones and inclusions) were selected for analysis. Analyzed multigrain fractions were homogeneous in terms of morphology, length/width ratio, colour and transparency. Most analyzed grains were air-abraded to remove zones of marginal lead loss. Prior to analysis, zircons were washed in warm 4N nitric acid and rinsed several times with distilled water and acetone in an ultrasonic bath. Dissolution and chemical extraction of U and Pb were performed following the method of KROGH (1973), using bombs and anion exchange columns that are scaled down to $^1/_{10}$ of their original size. Total procedural blanks usually are between 0.8 and 2 pg Pb and 0.1 pg U. Mass spectrometry and data reduction were done in the same way as described in SCHALTEGGER and CORFU (1995). The analytical data are compiled in table 2. Cathodoluminescence imaging of zircons was carried out on a CamScan scanning electron microscope equipped with a cathodoluminescence detector in order to gain additional information on growth conditions of the zircons.

Sm–Nd whole rock determinations: Samples of c. 150 mg whole-rock powder were attacked with HF + HNO$_3$ in Savillex® screw top containers after addition of a mixed ^{150}Nd–^{149}Sm tracer. After 24 hours, the acids were evaporated and the residue again attacked with HF + HNO$_3$. The closed vials were put on a hotplate at 150 °C for at least one week and repeatedly treated in an ultrasonic bath during this period. After evaporation, the samples were redissolved in 6N HCl. Chemical procedure and mass-spectrometry are described in NÄGLER et al. (1995). Nd ratios were normalized to ^{146}Nd/^{144}Nd = 0.7219. The mean value for the La Jolla standard during the period of measurement was 0.511870 for ^{143}Nd/^{144}Nd, with a 2σ external reproducibility of ± 0.000028 (10 measurements). Total chemistry blank is below 170 pg for Nd.

4. Geochemical characterization

Chemical analyses of major and trace elements of samples investigated by Sm–Nd and U–Pb are listed in table 1, except for ST 137, which was not analyzed because of heterogeneity and coarse grainsize. The full geochemical data set comprises some 150 samples, which will be published elsewhere by Maggetti because their discussion would clearly be beyond the scope of this paper. The analyzed rocks are polymetamorphic and MAGGETTI et al. (1987) presented evidence for element mobility. Ti, P, Y, Zr and REE were found to be relatively immobile elements and may be used for the comparison of geochemical trends.

In a Ti versus Zr diagram (Fig. 2) the gabbros display typical tholeiitic evolution trends characterized by an increase in Ti during the early stages of differentiation, due to removal of olivine, clinopyroxene and minor plagioclase. Of the whole data set of some 40 gabbro analyses, only a fraction of 6 samples represent basic liquids in the sense of PEARCE (1983), which does not allow any crystallization-fractionation modelling. MAGGETTI et al. (1990; Fig. 1) plotted these six non-cumulative gabbros in different diagrams involving V, Ti, Zr, Cr and Y and pointed out that the gabbros plot into the MORB field, where the island-arc and within-plate basaltic fields overlap. Contamination and/or fractionation effects have to be responsible for the shift from the IAB into the
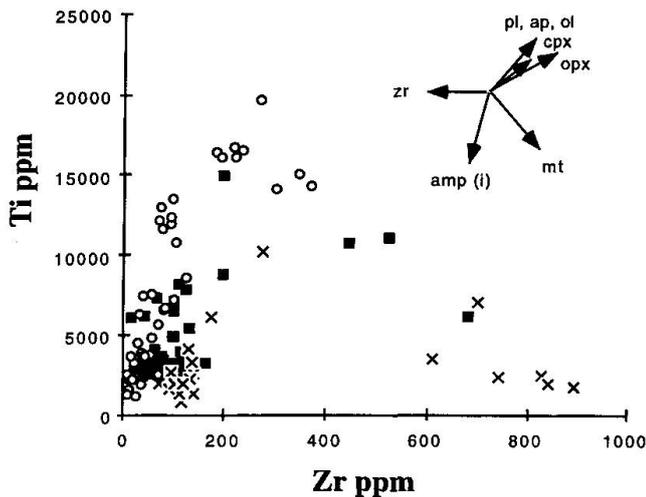
Fig. 2 Ti–Zr plot of 106 basic and intermediate older orthogneisses (circles: 40 gabbros, filled squares: 50 metadiorites, crosses: 26 metatonalites; MAGGETTI, unpublished data). Fractionation vectors after PEARCE and NORRY (1979) for basic magmas; ap: apatite; cpx: clinopyroxene; mt: magnetite; ol: olivine; opx: orthopyroxene; pl: plagioclase; zr: zircon; amp: amphibole; (i) represents a fractionation trend in intermediate magmas.

Fig. 3 N-MORB normalized spider diagrams; (a) for metagabbros and metadiorites (MAGGETTI, unpublished data); (b) for metatonalites (MAGGETTI, unpublished data) and eclogites (MAGGETTI et al., 1987).

Tab. 2   U–Pb age determinations of zircons.

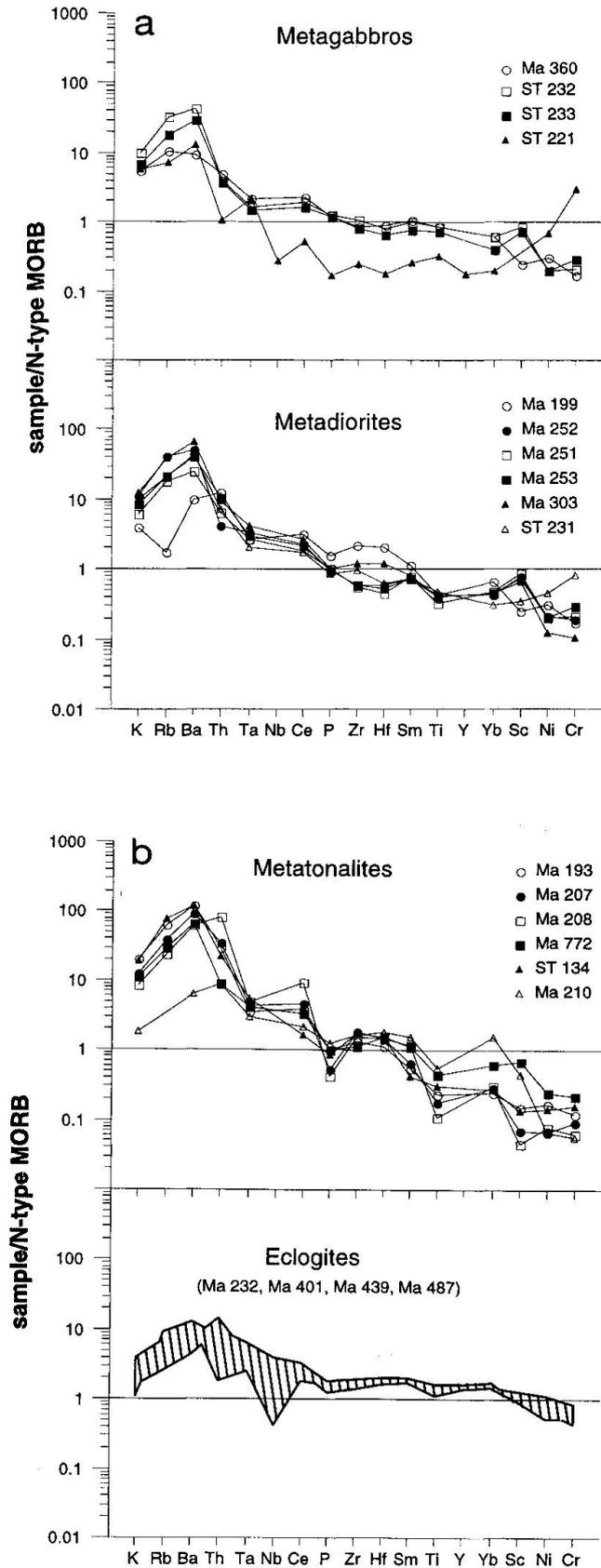| Nr.	Description a)	Weight [mg]	Nr. of grains	Concentrations [ppm]			Nonrad. Pb [pg]	Th/U b)	206/204 c)	Atomic ratios						Apparent ages			Error corr.
				U	Rad.Pb	Th b)				206/238 d)	Error 2s[%]	207/235 d)	Error 2s[%]	207/206 d)	Error 2s[%]	206/238	207/235	207/206	
Metadiorite, Val Lavinuoz (KAW 2886)																			
1	anh frags	0.03	17	223	25.31	206	1.6	0.92	25355	0.09720	0.47	0.80465	0.53	0.06004	0.15	598	599	605	0.96
2	euh pr	0.001	1	319	35.81	279	1.0	0.88	1926	0.09737	0.54	0.80880	0.94	0.06024	0.74	599	602	612	0.62
3	euh (-subh) pr	0.004	1	155	18.06	130	5.4	0.84	714	0.09738	0.48	0.80530	0.78	0.05998	0.54	599	600	603	0.73
4	euh (-subh) spr	0.016	6	568	64.50	512	1.2	0.90	48344	0.09768	0.46	0.80803	0.52	0.05999	0.15	601	601	603	0.96
5	euh spr non abr	0.015	14	1461	157.86	1259	3.3	0.86	39690	0.09403	0.32	0.77501	0.34	0.05978	0.11	579	583	596	0.95
Metatonalite, Val Sarsura (KAW 2874)																			
6	euh pr	0.003	1	683	53.06	88.5	0.6	0.13	16283	0.08226	0.47	0.65481	0.52	0.05773	0.17	510	511	520	0.95
7	euh eq	0.003	1	499	39.17	70.3	0.6	0.14	11965	0.08287	0.48	0.66021	0.54	0.05778	0.21	513	515	522	0.92
8	subh spr	0.003	7	289	23.74	84.6	1.5	0.29	2942	0.08294	0.49	0.66182	0.61	0.05787	0.33	514	516	525	0.84
9	small euh (-subh) spr	0.002	11	940	72.88	108	0.7	0.12	13504	0.08242	0.46	0.65565	0.52	0.05770	0.17	511	512	518	0.95
10	euh pr	0.004	1	271	21.29	48.4	2.4	0.18	2331	0.08156	0.46	0.64931	0.60	0.05774	0.30	505	508	520	0.87
11	subh cracks non abr	0.018	10	934	69.51	101	3.8	0.11	22187	0.07924	0.27	0.62914	0.31	0.05758	0.10	492	496	514	0.95
Coarse-grained metagabbro, Val Sarsura (KAW 2868)																			
12	frags	0.042	20	500	43.72	260	1.2	0.52	88842	0.08298	0.66	0.66009	0.68	0.05770	0.11	514	515	518	0.99
13	euh pr	0.028	12	465	40.05	214	1.2	0.46	55019	0.08306	0.48	0.66025	0.54	0.05766	0.10	514	515	517	0.99
14	euh and frags	0.027	8	838	72.95	417	0.8	0.50	143683	0.08307	0.56	0.66152	0.58	0.05776	0.09	514	516	521	0.99
15	frags	0.025	25	617	53.89	309	3.0	0.50	26513	0.08321	0.49	0.66154	0.56	0.05766	0.15	515	516	517	0.97
16	frags and euh non abr	0.019	10	2591	231.87	1656	1.7	0.64	149850	0.08234	0.29	0.65484	0.32	0.05768	0.10	510	511	518	0.95
Flasergabbro, Val Sarsura (KAW 2865)																			
17	euh and frags clear pink	0.02	10	947	78.71	331	1.5	0.35	67322	0.08262	0.56	0.65659	0.60	0.05764	0.11	512	513	516	0.98
18	euh pr	0.002	4	808	65.99	232	1.3	0.30	6611	0.08260	0.46	0.65820	0.56	0.05779	0.22	512	514	522	0.93
19	euh and frags	0.009	8	698	59.17	277	0.7	0.40	46289	0.08320	0.48	0.66170	0.53	0.05768	0.16	515	516	518	0.95
20	frags	0.01	17	520	44.02	229	4.0	0.44	6694	0.08178	0.49	0.64934	0.54	0.05759	0.20	507	508	514	0.93
21	euh tip pink non abr	0.006	1	1718	145.64	703	0.6	0.41	92047	0.08287	0.47	0.65933	0.54	0.05770	0.14	513	514	519	0.97
22	frags	0.003	5	999	86.49	487	0.5	0.49	30309	0.08287	0.47	0.65927	0.53	0.05770	0.16	513	514	518	0.96
Gabbro pegmatite, Val Sarsura (ST 137)																			
23	euh) spr pink Split A	0.132	11	84.4	6.11	10.0	1.5	0.12	35981	0.07684	0.47	0.60457	0.52	0.05706	0.15	477	480	494	0.96
24	dito Split B	0.132	11	84.5	6.12	10.1	2.2	0.12	24488	0.07688	0.46	0.60523	0.53	0.05710	0.17	477	481	495	0.95
25	frag red	0.004	1	4375	301.23	255	1.7	0.06	49108	0.07451	0.50	0.58008	0.56	0.05646	0.15	463	465	471	0.97
26	shells	0.001	2	79.2	5.49	1.26	1.3	0.02	314	0.07603	0.70	0.59801	2.94	0.05705	2.70	472	476	493	0.45
27	tip pink	0.001	1	3091	215.35	213	1.2	0.07	12354	0.07513	0.47	0.58641	0.53	0.05661	0.18	467	469	476	0.94
28	tip euh	0.003	1	52.5	3.65	1.78	1.0	0.03	753	0.07602	0.56	0.58528	1.60	0.05584	1.42	472	468	446	0.48
29	tip pink	0.001	1	1519	108.81	200	1.3	0.13	6693	0.07585	0.48	0.59264	0.55	0.05667	0.21	471	473	479	0.93

a) anh = anhedral; euh = euhedral; subh = subhedral; eq = equant; non abr = non abraded; pr = prismatic; frags = fragments; spr = short prismatic
b) Calculated on the basis of radiogenic $^{208}Pb/^{206}Pb$ ratios, assuming concordancy
c) Corrected for fractionation and spike
d) Corrected for fractionation, spike, blank and common lead (Stacey & Kramers, 1975)

MORB field, because a MOR setting is not substantiated by the spidergrams (Fig. 3) nor by the isotopic results (see below and KÖPPEL et al., this vol.). The Zr-rich metatonalites correspond to the garnet-plagioclase-hornblende-gneisses (meta-plagiogranites) of MÜLLER et al. (1996). Their geochemical trend may be explained by the removal of crystallizing magnetite and thus agrees with the hypothesis of MÜLLER et al. (1996) that they might represent late stage differentiation products of the gabbro melts.

Some metadiorites follow a similar, however distinct, tholeiitic evolution trend, but the majority of these rocks join the Ti- and Zr-poor metatonalites possibly following a poorly defined calc-alkaline trend. The geochemical characteristics of immobile elements thus do not allow discrimination between three rock series of different origin and/or age, i.e. metadiorites, metagabbros and metatonalites.

Multi-element, N-MORB-normalized plots (PEARCE, 1982) for selected samples of the OOG (tonalites, gabbros and diorites) show enrichment in LILE relative to N-MORB and negative HFSE anomalies in the metatonalites (Fig. 3), character-

istic for melts formed in island arc and at continental margin settings. Variation in LILE and LREE as a result of post-crystallization mobility affecting minerals like feldspars or apatite may be ruled out, because in all analyzed samples the degree of enrichment is of comparable magnitude; some variation may result from cumulation (e.g. gabbro ST 221). The eclogites are quite distinct from the mafic older orthogneisses, therefore pointing to a different genesis, i.e. crystallization as mafic liquids in an extensional oceanic setting (MAGGETTI et al., 1987; MAGGETTI and GALETTI, 1988). A slight LILE enrichment, however, can be observed in these rocks, suggesting the presence of slab-derived components in the upper mantle source region yielding transitional (T-type) MORB's.

The REE-plots (Fig. 4) show the transitional MORB-type pattern of the eclogites with small negative Eu anomalies due to crystallization and removal of plagioclase (data in MAGGETTI et al., 1990; MÜLLER et al., 1996). The coarse-grained gabbros and flasergabbros are characterized by a strong positive Eu anomaly which cannot be explained by plagioclase accumulation, as associated ultramafic cumulates display the same positive anomaly (MAGGETTI et al., 1990). Metatonalite ST 134, which is similar to metatonalite KAW 2874 and characteristic for the tonalites associated with the gabbros in Val Sarsura, shows a marked positive Eu anomaly. This rather unusual chemical behaviour is thus inherited from a plagioclase-enriched mantle reservoir (NORRY et al., 1980; DAVIES and MACDONALD, 1987). The LREE enrichment and the overall low REE contents of the metatonalites, however, indicate that they cannot be a differentiation product of the gabbroic melts because the differentiation products should have higher REE concentrations. Different tonalitic rocks show highly variable degrees of LREE enrichment (e.g. in MAGGETTI et al., 1990) and thus are a chemically heterogeneous rock group. The geochemical composition of metadiorite Ma 252, which closely resembles KAW 2886, clearly contrasts with the gabbros, showing no positive Eu anomaly and a steep LREE pattern. The absence of geochemical relationship is consistent with the 90 myr age difference between the two units.

In summary, these results as well as the data of SCHMID (1992) and BERLEPSCH (1996) suggest contrasting source regions for the precursor melts of the older orthogneisses, all generated in a volcanic arc environment with minor, co-magmatic differentiation trends on a very local scale.
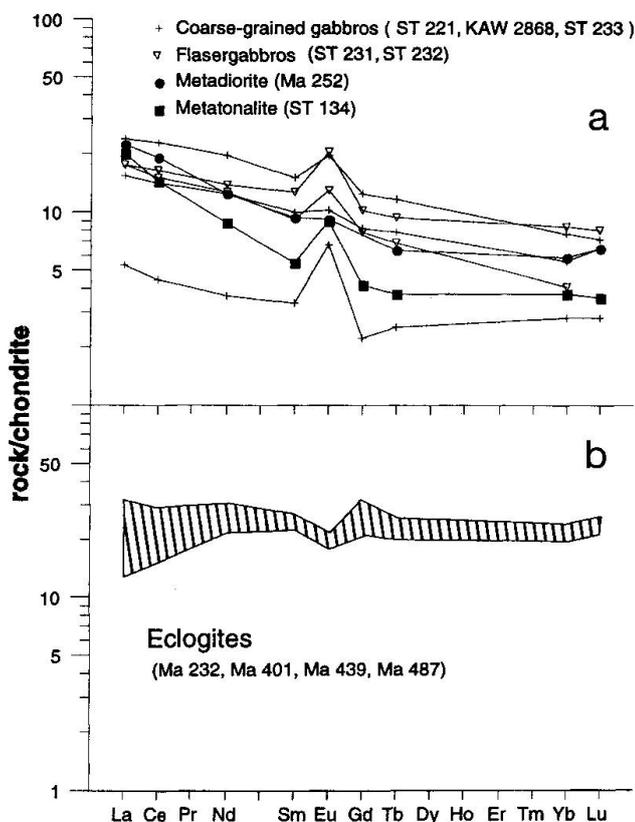

Fig. 4   Chondrite normalized REE patterns (a) for representative samples of metagabbros, metatonalite and metadiorite (MAGGETTI, unpublished data); (b) for eclogites (MAGGETTI et al., 1987). For normalization the recommended values of BOYNTON (1984) were used.
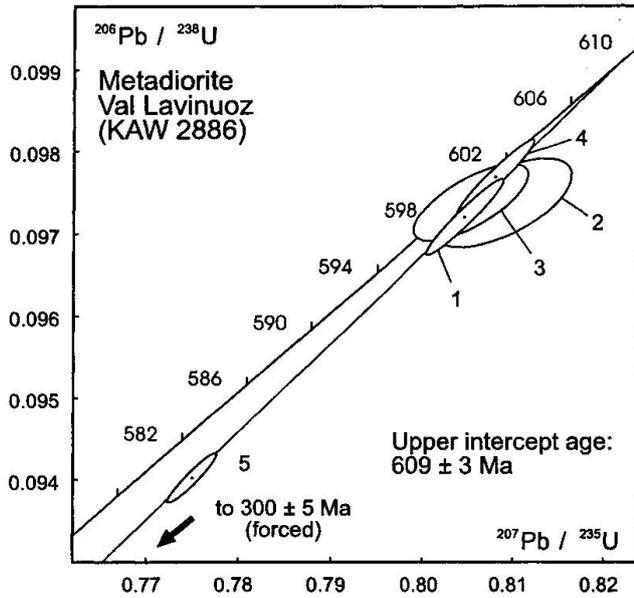
Fig. 5   U–Pb concordia diagram of a metadiorite from Val Lavinuoz; lower intercept has been forced through a Variscan age of 300 ± 5 Ma.

5. U–Pb age determinations of zircons (Tab. 2)

Metadiorite, Val Lavinuoz (KAW 2886; Fig. 5): Nonmagnetic zircons of this sample are mostly colourless and short prismatic and only rarely sharply facetted; most grains show rounded edges. Large reddish fragments are paramagnetic and have incorporated inclusions and turbid zones, thus not suitable for analysis. CL imaging revealed undisturbed magmatic zoning patterns and thin low-U rims that may be assigned to metamorphic overgrowth. The latter were removed by abrasion. Three fractions and two single grains were analyzed from this rock; analyses 1 to 4 with U concentrations of 160 to 570 ppm are subconcordant at an U–Pb age of 600 Ma, whereas a non-abraded fraction of 14 U-rich zircons (5) is strongly discordant. The spread of data points is dominated by analysis 5 and too small to compute a meaningful lower intercept age; a best-fit line with a MSWD value of 1.09 is therefore forced through a Variscan intercept of 300 ± 5 Ma, a value estimated from the data of LIEBETRAU et al. (1996; 301 ± 3 Ma) and FREI et al (1996; 306 ± 8 and 304 ± 6 Ma), which results in an upper intercept age of 609 ± 3 Ma.

Coarse-grained metagabbro, Ova Sparsa, Val Sarsura (KAW 2868; Fig. 6a): This sample shows mostly anhedral or fragmented zircons, typical for gabbroic lithologies. U concentrations of colourless abraded zircons are between 700 and 1000 ppm; an unabraded fraction (16) showing pink
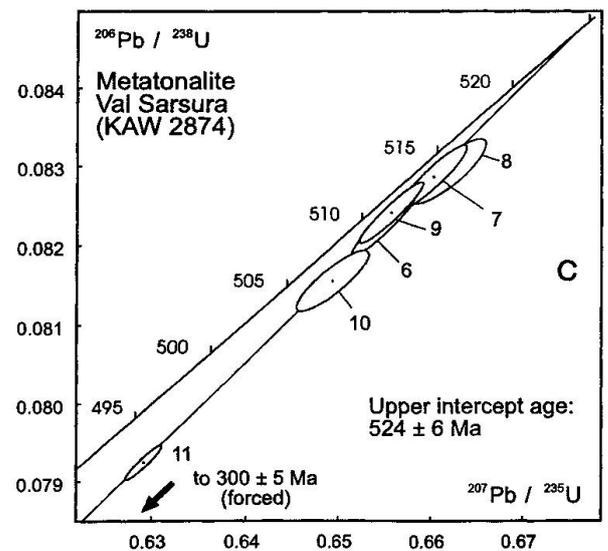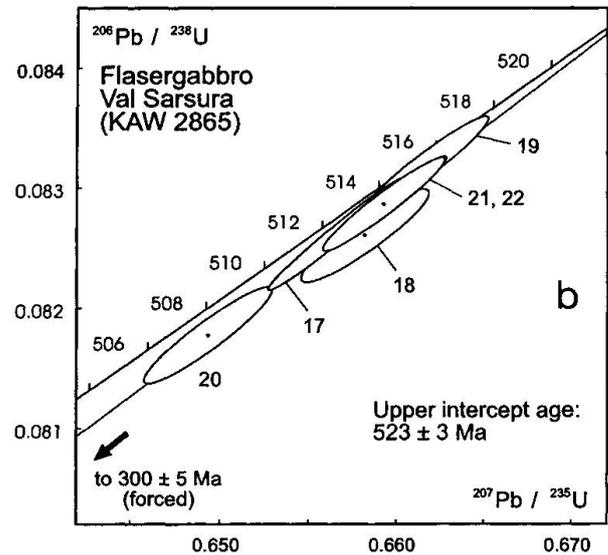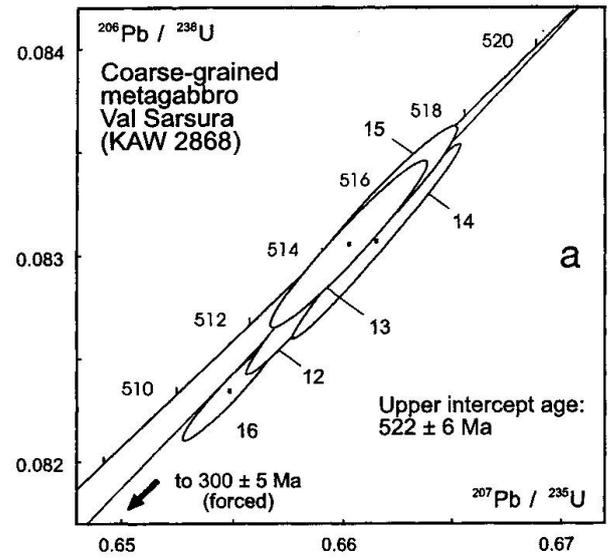

Fig. 6   U–Pb concordia diagrams of (a) metagabbro, (b) flasergabbro and (c) metatonalite from Val Sarsura. Lower intercepts have been forced through 300 ± 5 Ma, except for metatonalite KAW 2874.

colour and turbid zones has a U content of 2600 ppm, but is only slightly more discordant than the other analyses. Analyses 12 to 14 yielded subconcordant results, which are identical within error margins. The mean $^{207}Pb/^{206}Pb$ age of 518 ± 4 Ma of the 5 analyzed fractions, however, is not regarded as best age estimate. Considering the lead loss in the zircons of other samples, especially of the flasergabbro KAW 2865, a Variscan age for the major proportion of lead loss seems more plausible. We therefore favour a best-fit line forced through an intersection at 300 ± 5 Ma, as best age estimate, yielding an upper intercept age of 522 ± 6 Ma (MSWD = 2.85), identical with the age of the metatonalite KAW 2874.

Flasergabbro, Ova Sparsa, Val Sarsura (KAW 2865; Fig. 6b): The zircons of this sample are not significantly different from those of the coarse-grained metagabbro, which is interpreted as being representative for the undeformed protolith of the flasergabbros. Analyses 17 to 22 show some scatter in their $^{207}Pb/^{206}Pb$ ratios; analysis 18 may be slightly influenced by a minor amount of inherited lead. A discordia line calculated with analyses 17 to 22 points to a lead loss of Variscan age (309 Ma) with an extremely high error on the upper intercept. The discordia has therefore been forced to a lower intersection at 300 ± 5 Ma yielding an upper intercept age of 523 ± 3 Ma (MSWD = 0.38). This age does not differ from the age of the undeformed gabbro (KAW 2868).

Metatonalite, Val Sarsura (KAW 2874; Fig. 6c): Most of the extracted zircons are strongly etched and no edges and tips are preserved but {211} faces are still recognizable. The U–Pb determinations straddle a best-fit line with an upper intercept age of 524 ± 6 Ma (MSWD = 0.57). Analysis 8 plots at a slightly higher $^{207}Pb/^{206}Pb$ ratio due to minor amounts of inherited lead, which is suggested by the occurrence of inherited cores in other grains of the population, visible in cathodo-luminescence. Since this deviation is not significant, the point has not been excluded from discordia calculation. The lower intersection at 175 ± 70 Ma points to a complex lead loss during Variscan and Alpine times.

Gabbro pegmatite, Val Sarsura (ST 137; Fig. 7): The zircons were hosted by large anhedral plagioclase crystals between pyroxene phenocrysts. The zircon population is heterogeneous with respect to colour, size and morphology. CL imaging revealed resorbed cores in relatively large crystals, overgrown by broad homogeneous high-Cl (low-U) zones and seldom by an outermost thin high-U rim. The U–Pb age determinations covered all different zircon types: a large fraction of euhedral and short prismatic low-U zircons yielded a dis-
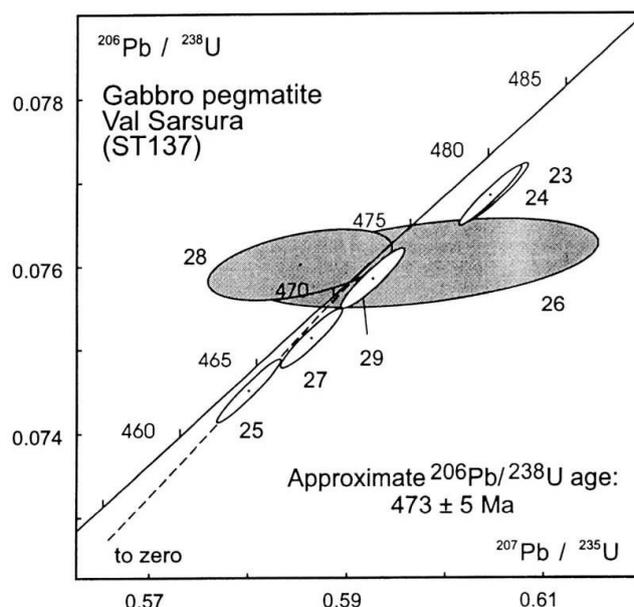

Fig. 7 U–Pb concordia diagram of the gabbro pegmatite ST 137 from Val Sarsura.

cordant result (duplicate mass spectrometer analyses 23 and 24) with a $^{207}Pb/^{206}Pb$ age of 495 Ma, suggesting that these are xenocrysts derived from the surrounding metagabbros. Colourless shells and tips broken off large zircon grains (26, 28, 29) are extremely low in U (50 to 80 ppm) and are concordant within analytical errors at a $^{206}Pb/^{238}U$ age of ca. 473 Ma with an estimated uncertainty of ± 5 Ma. Red- to pink-coloured fragments and tips of euhedral zircons (25, 27) have high concentrations of up to 4300 ppm U and plot slightly discordant at $^{206}Pb/^{238}U$ ages of 463 to 471 Ma, pointing to a small contribution of inherited lead. The best estimate for the intrusion of this pegmatite is 473 ± 5 Ma, thus being 50 myr younger than the formation of the gabbro intrusions.

6. Sm–Nd whole-rock isotope determinations

Six samples have been analyzed for Sm–Nd (see Tab. 3, Fig. 8). Nd concentrations vary between 9 and 16 ppm, a typical range for mafic crustal rocks. The $^{147}Sm/^{144}Nd$ ratios (0.155–0.190) are typical for mafic rocks in crustal environments with the exception of KAW 2874. They yield Nd depleted mantle model ages (T_{DM}) around 0.95 Ga, except for metatonalite KAW 2874, with a one-stage T_{DM} model age of 0.73 Ga and a much lower $^{147}Sm/^{144}Nd$ ratio of 0.116. It is suggested that its lower $^{147}Sm/^{144}Nd$ ratio results from REE fractionation related to the intrusion of the magma at 520 Ma and that its precursor/source evolved be-

Tab. 3   Sm–Nd isotopic results.

Lithology	Number	Sm (ppm)	Nd (ppm)	$^{147}Sm/^{144}Nd$	$^{143}Nd/^{144}Nd$	± 2σ	$\varepsilon_{Nd}(0)$	$\varepsilon_{Nd}(T)$ (a)	$T_{DM}(Ga)$ (b)
Metagabbro	KAW 2865	2.9	11.3	0.1553	0.512741	0.000019	2.0	4.8	0.99
Metagabbro	KAW 2868	3.5	13.5	0.1550	0.512757	0.000048	2.3	5.1	0.95
Metagabbro	KAW 2887	2.7	9.4	0.1723	0.512823	0.000042	3.6	5.2	1.07
Metatonalite	KAW 2874	1.4	7.4	0.1162	0.512671	0.000026	0.6	6.0	0.95
Metadiorite	KAW 2886	3.3	11.7	0.1678	0.512851	0.000039	4.2	6.4	0.91
Eclogite	KAW 2879	4.9	15.6	0.1897	0.512974	0.000023	6.6	7.1	0.94

(a) Corrected for the intrusion age of 520 Ma for all samples except KAW 2886 (600 Ma) and 2879 (620 Ma).
(b) Depleted mantle model ages T_{DM} are calculated relative to the depleted mantle model evolution of NÄGLER and KRAMERS (1997). For KAW 2874 a two-stage calculation was applied, adapting a $^{147}Sm/^{144}Nd$ ratio of 0.17 for the extrapolation from 520 Ma.

fore under a $^{147}Sm/^{144}Nd$ ratio representative for the whole suite (0.17). Applying the latter ratio of 0.17 results in a two-stage model age of 0.95 Ga, equal to the mafic rocks (curve 2874/2 on Fig. 8).

Initial ε_{Nd} values of OOG samples at the age of intrusion (520 or 608 Ma, respectively) are all in the very narrow range between +4.8 and +6.4 and all overlap within analytical precision. Eclogite KAW 2879 is, however, slightly higher at a value of +7. All ε_{Nd} are significantly below a model value for depleted mantle at 520 Ma (ca. +9 according to NÄGLER and KRAMERS, 1997, or GOLDSTEIN et al., 1984) and point to a low-Sm/Nd mantle source.

7. Discussion

The U–Pb age determinations record three important episodes of magmatic activity at ca. 610, 525 and 475 Ma. The 609 ± 3 Ma age for the Val
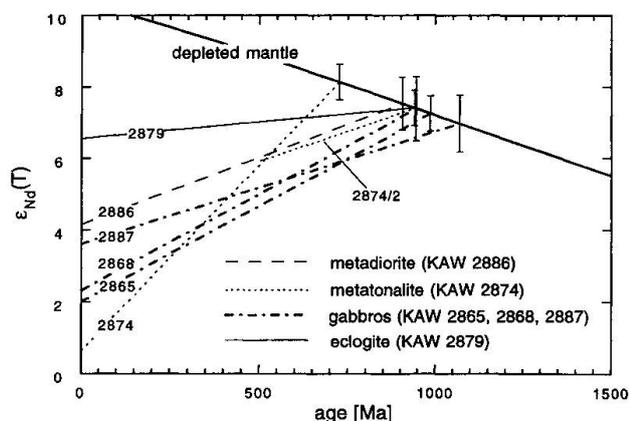

Fig. 8   Sm–Nd evolution diagram for six samples of the Older Orthogneisses. Line 2874/2 represents a two-step model assuming fractionation of the Sm/Nd ratio at the time of intrusion and a $^{147}Sm/^{144}Nd$ ratio typical for the whole suite (0.17) has therefore been taken to extrapolate back to the mantle line.

Lavinuoz metadiorite is among the oldest protolith ages presently known from the Alpine basement. The extrusion/intrusion of the widespread MORB-type basaltic melts (now eclogitic and amphibolitic metabasites) might hypothetically relate to this age, too, or may be slightly older; VON QUADT (1992) reported ages of 657 ± 15 and 640 ± 7 Ma for banded amphibolites of the Tauern Window. The age of the HP metamorphism forming the eclogite mineral assemblage remains enigmatic. The Cambrian magmatic event with a mean age of 525 ± 5 Ma seems well documented by our data and age determinations of MÜLLER et al. (1995; 523 ± 7 Ma for a metagranitoid Kfs-gneiss; 533 ± 4 Ma for a metatonalite), MÜLLER et al. (1996; 523 ± 30 Ma for a garnet-hornblende-plagioclase gneiss with a plagiogranite protolith) and LIEBETRAU et al. (1996; 527 ± 4 Ma for an S-type granitoid, the so-called Mönchalp augengneiss), as well as by data of MILLER and THÖNI (1996; 521 ± 10 to 530 ± 2 Ma-old gabbros from the Ötztal basement). The magmatic activity at that time occurred in oceanic as well as continental geodynamic environments, represented by the variety of granitoid rocks ranging from plagiogranites to crustal anatexites. The 475 Ma event is reflected by the pegmatoid gabbro dike from Val Sarsura (ST 131) but has also been found in gabbro intrusions from the Val Barlas-ch a few km further south (POLLÈR, this volume). Ordovician ages have also been determined on oceanic rocks from the Aar and Gotthard massifs (ABRECHT et al., 1995; OBERLI et al., 1994).

The metabasites, metadiorites, metatonalites, Mönchalp augengneisses and flasergabbros contain high-pressure mineral assemblages. The flasergabbros are considered to have formed in shear-zones within the gabbro protoliths, which preserved the magmatic texture in less deformed rock portions. Age determinations of the gabbro types agree at 522 Ma, which leaves two interpre-

tations: either the intrusion and crystallization occurred under HP shearing conditions, or the HP overprint took place later along shear zones with fluid influx and did not affect the zircon U–Pb systematics.

The ε_{Nd} data of gabbro and tonalite samples scatter in a very narrow range of 4.8–6.0 at 520 Ma, indicating little variation of source compositions and contamination. Crustal contamination of gabbros and tonalites is clearly reflected by the presence of amphibolite and gneiss xenoliths and was modelled by using Nd isotopic data. Assuming a MORB-type mantle endmember with ε_{Nd} (520 Ma) = +8.8 and 8 ppm Nd, and a crustal endmember with 26 ppm Nd and a Nd model age of 1.7 Ga, typical for average Mönchalp gneiss (POLLER et al., 1997), a proportion of 10% crustal contaminant can be computed. This estimate has to be considered as a maximum, because it may be decreased by assuming a mantle component less depleted than MORB, which seems to be more probable (see discussion below) and also by concurrent fractional crystallization (AFC). The value of < 10% compares very well with 5% crustal contaminant derived from Pb isotopes from a source with the same Pb isotopic composition as the Silvretta paragneisses (KÖPPEL et al., this volume). A slightly elevated initial Sr isotopic ratio of 0.7036 of metatonalites and metagabbros might be related to this minor crustal contamination, too. High initial $^{87}Sr/^{86}Sr$ values of meta-plagiogranites (biotite-hornblende-plagioclase gneisses) around 0.707 (data from MÜLLER et al., 1996), on the other hand, could possibly be explained by sea-floor alteration, since crustal contamination should be subordinate in oceanic rocks.

The major question to discuss is the geochemical composition of the hypothetical mantle source. The narrow range in ε_{Nd} at values of +4.8 to +6.0 rather indicates a less-depleted mantle source than a MORB-type reservoir. A LREE-enriched mantle segment that is presently underlying European continental crust has ε_{Nd} values between +3.5 and +6 and may serve as a model for the source of the mafic Silvretta OOG (STILLE and SCHALTEGGER, 1996). If we adopt this mantle model, even less than the proposed maximum of 10% crustal contamination is required for metagabbros and metatonalites to arrive at ε_{Nd} values of +4.8 to +6. It is, however, highly unusual for arc magmas to tap ancient lithosphere as a source.

8. Geodynamic scenario (Tab. 4)

The OOG of the Silvretta nappe represent a rock suite derived from one or several late Proterozoic to Early Cambrian island arc(s). From geochemical and isotope constraints we can infer five different components present within this arc:

(a) A depleted, MORB-type asthenospheric mantle is assumed to be the source for the metabasites (eclogites, amphibolites) that show T- to P-type MORB characteristics.

(b) A less depleted mantle component, enriched in LILE and LREE compared to the latter, is proposed as source of the gabbroic and tonalitic OOG melts.

(c) The 610 Ma-old metadiorites represent an older generation of intrusive or extrusive island-arc magmatites, which intruded into or extruded onto a preexisting arc-type crust.

(d) Plagiogranites occurring in contact to the metagabbros are considered to be part of dismembered ophiolitic sequences (MÜLLER et al., 1996). Ophiolites are common in back-arc envi-

Tab. 4 Synopsis: Cambrian-Ordovician evolution of the Silvretta Nappe.

pre-609 Ma	? Oceanic sedimentation and basaltic MOR-type volcanism; continental detritus of Cadomian to early Proterozoic age (Gondwana affinity)
609 ± 3 Ma	Intermediate magmatism in a volcanic arc environment
609 to 530 Ma	Docking of the 609 Ma-old arc-type crust against a continent (Laurasia)
530 to 520 Ma	? Closing of the oceanic realm; acid magmatism on the continent (S-type granites); intrusion of gabbroic and tonalitic melts in an arc environment, probably a continental margin magmatic arc
	Formation of oceanic plagiogranites either in a back-arc of fore-arc environment
post-520 Ma; pre-475 Ma	Tectonic mélange of continental and oceanic tectonic units during collision and orogenesis in the Ordovician
475 Ma	Intrusion of gabbroic melts into a collisional belt, reheating the crust (POLLER, this vol.)
ca. 460–420 Ma	Acid S-type granitoid plutonism on this continent (LIEBETRAU, 1996); Younger Orthogneisses

ronments and often associated with neighbouring island-arcs. Coeval oceanic assemblages of this type are well known from many different places within the Alpine basement (e.g. Chamrousse; MÉNOT et al., 1988; Cima di Gagnone, GEBAUER, 1996).

(e) An old continental mass occurred in the neighbourhood of the island arc because it influenced the arc magmas to some extent. High T_{DM} model ages up to 1.7 Ga for the metasedimentary sequences as well as for the S-type granitoids (BIINO et al., 1994; POLLER, 1994b, 1997) and Pb inheritance in zircon (GRAUERT and ARNOLD, 1968) testify that this continental source had Early Proterozoic components.

The 610 Ma age for KAW 2886 metadiorite is a common age for Pb inheritance in zircons of rhyolites, granites and gneisses of the Variscan belt. It is a typical age representing the formation of protoliths in a juvenile "European" crust, which may have been formed in a (more primitive than present-day) Japan-type arc. Island arc rocks with ages between ca. 620 and 480 Ma infer a long-lived oceanic basin off the Gondwana continent. The lifetime of this ocean started at the onset of peripheral break-up of the Gondwana margin and lasted until the different microcontinents and island arcs collided with the Laurasia continental margin during the Ordovician to Silurian orogeny.

The hypothetical continental mass inferred from the geochemical contamination of arc magmas as well as from the existence of granitoid plutonic rocks is supposed to be mainly of Cadomian age, with some zircon inheritance up to Archean age. Remnants of this Cadomian orogenesis would be expected to yield ages around 590 to 530 Ma (e.g. KRÖNER et al., 1994). The precursor rocks of Mönchalp granitoids as well as the alkali granite of MÜLLER et al. (1995) formed within this age range. The gabbroic melts intruded into metamorphic continental sequences consisting of amphibolites and metasediments 520 Ma ago.

All these rocks form a magmatic arc either situated at an active continental margin or in a back-arc setting. In both settings crustal contamination of the gabbroic melts and coexistence of arc-type and oceanic rock associations would have been possible. The rocks became subsequently involved in orogenic processes in the Ordovician (475 Ma), during which the mafic and intermediate "oceanic" OOG were tectonically intermingled with the acid granitoid OOG and were intruded by a younger generation of 475 Ma-old gabbroic melts. We prefer not to call this latter orogeny "Caledonian", as this term could be misunderstood as genetically relating to the Caledonides of northern Europe. The Ordovician-Si-lurian orogenic processes in the Silvretta nappe were terminated by the last intrusions of late-orogenic granitoids ca. 420 Ma ago (LIEBETRAU, 1994) and are thus coeval to other orogenic suites from the central and southern Alpine domains.

The new data presented in this study provide more evidence for the existence of a Cambrian ocean separating the two continental blocks of Gondwana and Laurasia. The oceanic basin contained volcanic arcs and microcontinents that rifted off the Gondwana continent after 610 Ma and were accreted to the Laurasia continental shelf during closure of this ocean basin and collision of the two continental blocks before 475 Ma.

Acknowledgements

References

ABRECHT, J., BIINO, G.G. and SCHALTEGGER, U. (1995): Building the European continent: Late Proterozoic – Early Paleozoic accretion in the Central Alps of Switzerland. EUG 8, Strasbourg. Terra abstracts 7/1: 105.

BENCIOLINI, L. (1994): Metamorphic Evolution of the Silvretta Gabbro and related rocks (Upper Austroalpine, Central Alps). Its bearing on the pre-Mesozoic history of the alpine area basement. Memorie di Scienze geologiche, 46, 353–371.

BERLEPSCH, P. (1996): Die Granitoide der Region Jakobshorn (Silvretta, Schweiz): Hinweise auf eine ozeanische Herkunft der "Meta-Aplite". Schweiz. Mineral. Petrogr. Mitt. 76, 209–216.

BIINO, G.G., MEISEL, TH., NÄGLER, TH. and KRAMERS, J. (1994): Whole-rock chemistry and isotope chemistry of metasediments in the Silvretta nappe and the early crustal history of the Alpine basement. Schweiz. Mineral. Petrogr. Mitt. 75, 293–294.

BOYNTON, W.V. (1984): Cosmochemistry of the rare earth elements: meteorite studies. In: HENDERSON, P. (ed.): Rare Earth Element Geochemistry. Elsevier, Amsterdam, 63–114.

DAVIES, G.R. and MACDONALD, R. (1987): Crustal influences in the petrogenesis of the Naivasha basalt – comendite complex: combined trace-element and Sr–Nd–Pb isotope constraints. J. Petrol. 28, 1009–1051.

FREI, R., BIINO, G.G. and PROSPERT, C. (1995): Dating a Variscan pressure-temperature loop with staurolite. Geology 12, 1095–1098.

GEBAUER, D. (1996): A P-T-t path for a (ultra?-) high-pressure ultramafic/mafic rock associations and their

felsic country-rocks based on SHRIMP-dating of magmatic and metamorphic zircon domains. Example: Alpe Arami (Central Swiss Alps). In: BASU, A. and HART, S.R. (eds): Earth Processes: Reading the Isotopic Code. Geophysical Monograph Series vol. 95, 307–329, Am. Geophys. Union, Washington.

GOLDSTEIN, S.L., O'NIONS, R.K. and HAMILTON, P.J. (1984): A Sm–Nd isotopic study of atmospheric dust and particulates from major river systems. Earth Planet. Sci. Lett. 70, 221–236.

GRAUERT, B. (1969): Die Entwicklungsgeschichte des Silvrettakristallins aufgrund radiometrischer Altersbestimmungen. Unpubl. Ph. D. Thesis, University of Bern.

GRAUERT, B. and ARNOLD, A. (1968): Deutung diskordanter Zirkonalter der Silvrettadecke und des Gotthardmassivs (Schweizer Alpen). Contrib. Mineral. Petrol. 20, 34–56.

HUIJSMANS, J.P.P. (1985): Calc-alkaline lavas from the volcanic complex of Santorini, Aegean Sea, Greece. A petrological, geochemical and stratigraphic study. Ph. D. Thesis, Geol. Ultraiectina 41.

KÖPPEL, V., HANSMANN, W. and MAGGETTI, M. (1997): Pb isotope and trace element signatures of polymetamorphic rocks from the Silvretta nappe, a comparison. Schweiz. Mineral. Petrogr. Mitt. 77, 325–335.

KRÖNER, A., HEGNER, E., HAMMER, J., HAASE, G., BIELICKI, K.-H., KRAUSS, M. and EIDAM, J. (1994): Geochronology and Nd–Sr systematics of Lusitanian granitoids: significance for the evolution of the Variscan orogen in east-central Europe. Geol. Rundschau 83, 257–376.

KROGH, T.E. (1973): A low contamination method for the hydrothermal decomposition of zircon and extraction of U–Pb for isotopic age determinations. Geochim. Cosmochim. Acta 37, 637–649.

LIEBETRAU, V., POLLER, U., TODT, W. and MAGGETTI, M. (1996): Geochronological studies on eclogites of the Silvretta Nappe / Central Alps. Mitt. Österr. Mineral. Ges. 141, 136–137.

LIEBETRAU, V. (1996): Petrographie, Geochemie und Datierung der Flüelagranitischen Assoziation (Jüngere Orthogneise) des Silvrettakristallins – Graubünden/Schweiz. Unpubl. Ph. D. Thesis, Univ. of Fribourg.

MAGGETTI, M. and FLISCH, M. (1993): Evolution of the Silvretta Nappe. In: VON RAUMER, J. and NEUBAUER, F. (eds): Pre-Mesozoic Geology in the Alps. Springer, Berlin-Heidelberg, 469–484.

MAGGETTI, M., GALETTI, G. (1988): Evolution of the Silvretta eclogites: metamorphic and magmatic events. Schweiz. Mineral. Petrogr. Mitt. 68, 467–484.

MAGGETTI, M., GALETTI, G., STOSCH, H.G. (1987): Eclogites from the Silvretta nappe (Switzerland): geochemical constraints on the nature and geotectonic setting of their protoliths. Chemical Geology, 64, 319–334.

MAGGETTI, M., GALETTI, G., STOSCH, H.G. (1990): Geochemische Argumente zur Genese der "Älteren Orthogneise" der Silvretta. Schweiz. Mineral. Petrogr. Mitt. 70, 103–107.

MÉNOT, R.P., PEUCAT, J.J., SCARENZI, D. and PIBOULE, M. (1988): 496 Ma age of plagiogranites in the Chamrousse ophiolitic complex (external crystalline massifs in the French Alps): evidence of a Lower Paleozoic oceanization. Earth Planet. Sci. Lett. 88, 82–92.

MILLER, CH. and THÖNI, M. (1996): Origin of eclogites from the Austroalpine Ötztal basement (Tirol, Austria): geochemistry and Sm–Nd vs Rb–Sr isotope systematics. Chem. Geol. (Isot. Geosci. Sect.), 122, 199–225.

MÜLLER, B., KLÖTZLI, U. and FLISCH, M. (1995): U–Pb and Pb–Pb dating of the older orthogneiss suite in the Silvretta nappe, eastern Alps: Cadomian magmatism in the upper Austro-Alpine realm. Geol. Rundschau 84, 457–465.

MÜLLER, B., KLÖTZLI, U., SCHALTEGGER, U. and FLISCH, M. (1996): Early Cambrian oceanic plagiogranite in the Silvretta Nappe, eastern Alps: geochemical, zircon U–Pb and Rb–Sr data from garnet-hornblende-plagioclase gneisses. Geol. Rundschau 85, 822–831.

NÄGLER, TH.F. and KRAMERS, J.D. (1997): Nd Isotopic Evolution of the Upper Mantle during the Precambrian: Models, data and the uncertainty of both. Precambrian Res., in press.

NÄGLER, TH.F., PETTKE, TH. and MARSHALL, D. (1995): Initial isotopic heterogeneity and secondary disturbance of the Sm–Nd system in fluorites and fluid inclusions: A study on mesothermal veins from the central and western Swiss Alps. Chem. Geol. 125, 241–248.

NORRY, M.J., TRUCKLE, P.H., LIPPARD, S.J., HAWKESWORTH, C.J., WEAVER, S.D. and MORRINER, G.F. (1980): Isotopic and trace element evidence from lavas, bearing on mantle heterogeneity beneath Kenya. Philos. Trans. R. Soc. London, A, 297, 251–271.

OBERLI, F., MEIER, M. and BIINO, G.G. (1994): Time constraints on the pre-Variscan magmatic/metamorphic evolution of the Gotthard and Tavetsch units derived from single-zircon U–Pb results. Schweiz. Mineral. Petrogr. Mitt. 74, 483–488.

PEARCE, J.A. (1982): Trace element characteristics of lavas form destructive plate boundaries. In: R.S. THORPE (ed.): Andesites: Orogenic Andesites and Related rocks, Wiley, New York, 525–548.

PEARCE, J.A. (1983): A "users" guide to basalt discrimination diagrams. Unpubl. Report. The Open University, Milton Keynes, 37 pp.

PEARCE, J.A. and NORRY, M.J. (1979): Petrogenetic implications of Ti, Zr, Y and Nb variations in volcanic rocks. Contrib. Mineral. Petrol. 69, 33–47.

POLLER, U. (1994a): Petrographie, Geochemie und Datierung der Augengneise Typ Mönchalp (Ältere Orthogneise) des Silvrettakristallins, Graubünden, Schweiz. Unpubl. Ph. D. Thesis University of Fribourg.

POLLER, U. (1994b): Der Mönchalpgneis der Silvrettadecke (Graubünden): Geochemie und Sm-Nd-Modellalter. Schweiz. Mineral. Petrogr. Mitt. 74, 269–272.

POLLER, U., NÄGLER, TH., LIEBETRAU, V. and GALETTI, G. (1997): Geochemical and Sm–Nd characteristics of a polymetamorphic S-type granitoid: The Mönchalpgneiss-Silvretta nappe/Switzerland. Eur. J. Min. 9, 411–422.

POLLER, U. (1997): U–Pb single zircon study of gabbroic and granitic rocks in the Val Barlas-ch / Silvretta nappe. Schweiz. Mineral. Petrogr. Mitt. 77, 351–359.

PROSPERT, C. (1996): Formation et évolution des veines et agrégats de quartz à Al_2SiO_5 de la Silvretta – Etude pétrostructurale et des inclusions fluides. Ph. D. Thesis Univ. of Freiburg, Switzerland.

VON QUADT, A. (1992): U–Pb zircon and Sm–Nd geochronology of mafic and ultramafic rocks from the central part of the Tauern Window (eastern Alps). Contrib. Mineral. Petrol. 110, 57–67.

SCHALTEGGER, U. and CORFU, F. (1995): Late Variscan "basin and range" magmatism and tectonics in the Central Alps: Evidence from U–Pb geochronology. Geodin. Acta 8, 82–98.

SCHMID, J. (1992): Petrographie und Geologie von Munt

(westlich Zernez, Engadin). Unpubl. Diploma Thesis, Univ. Fribourg, Switzerland.

SPAENHAUER, F. (1932): Petrographie und Geologie der Grialetsch-Vadret-Sarsura-Gruppe, GR. Schweiz. Mineral. Petrogr. Mitt. 12, 27–146.

STACEY, J.S. and KRAMERS, J.D. (1975): Approximation of terrestrial lead isotope evolution by a two-stage model. Earth Planet. Sci. Lett. 26, 207–221.

STILLE, P. and SCHALTEGGER, U. (1996): The lithospheric mantle beneath Central Europe: Nd isotopic constraints for its Late Proterozoic enrichment and implications for early crustal evolution. In: BASU, A. and HART, S.R. (eds): Earth Processes: Reading the

Isotopic Code. Geophysical Monograph Series vol. 95, 269–276, Am. Geophys. Union, Washington.

THIERRIN, J. (1982): Géologie et pétrographie du val Sarsura, Grisons. Unpubl. Diploma Thesis, University of Fribourg.

THIERRIN, J. (1983): Les éclogites et le complexe gabbroïque du Val Sarsura (Silvretta). Schweiz. Mineral. Petrogr. Mitt. 63, 479–496.